BOLLETTINO DI GEOFISICA TEORICA ED APPLICATA VOL. 40, N. 1, pp. 19-30; MARCH 1999

A method for estimating gas hydrate and free gas concentrations in marine sediments

U. TINIVELLA

Osservatorio Geofisico Sperimentale, Trieste, Italy

(Received January 14, 1999; accepted April 30, 1999)

Abstract. I propose a method for estimating gas hydrate and free gas concentrations versus depth in marine sediments, using Gassmann's equation. The theory models gas hydrate- and free gas-bearing sediments partially saturated with water. A qualitative estimate of the concentrations can be obtained by comparing the theoretical velocity for full-water saturation to the experimental velocity, evaluated by a tomographic analysis or available from well logging. Positive anomalies indicate the presence of gas hydrate and negative anomalies indicate the presence of free gas. A quantitative estimate of concentrations is obtained by fitting the theoretical velocity to the experimental velocity. The method has been tested against sonic log and VSP data and indirect estimations of gas hydrate concentration from chloride content in core logs.

1. Introduction

Gas hydrates (a type of chlatrates) area solid phase composed of water and low-molecular-weight gases (predominantly methane) which form under low temperature, high pressure, and adequate gas concentrations. These conditions are common in the upper few hundred meters of rapidly accumulated marine sediments (Claypool and Kaplan, 1974).

The presence of gas hydrates in marine sediments is generally related to the so-called Bottom Simulating Reflectors (BSR), a seismic event that mimics the relief of the sea floor. These reflections mark the pressure- and temperature-dependent base of the methane-hydrate stability field (e.g., Shipley et al., 1979). BSR's have high-amplitudes, and are associated with a phase reversal (Shipley et al., 1979), caused by the strong acoustic impedence contrast between the hydrate-bea-

Corresponding author: U. Tinivella; Osservatorio Geofisico Sperimentale, P.O. Box 2011 Opicina, 34016 Trieste, Italy; tel: +39 040 2140341; fax: +39 040 327307; e-mail: utinivella@ogs.trieste.it

ring sediments and the underlying free gas layer.

The elastic properties of ice are similar to those of hydrate, so the properties of permafrost are often compared with those of hydrated sediments (Sloan, 1990). Timur (1968) proposed a three-phase time-average equation based on slowness averaging (Wyllie's equation) for modelling consolidated permafrost sediments. The problem of transition from "suspension to compacted" sediment was treated with combined models. For instance, averaging bulk moduli weighted with the respective porosities (Voigt's model; Voigt, 1928) gives a simple model for consolidated sediments, while averaging the reciprocal of bulk moduli (Reuss's model; Reuss, 1929) accounts for unconsolidated media. Zimmerman and King (1986) used the two-phase theory developed by Kuster and Toksöz (1974), assuming that unconsolidated permafrost can be approximated by an assemblage of spherical quartz grains imbedded in a matrix composed of spherical inclusions of water and ice. Minshull et al. (1994) obtain an effective medium 1 by time averaging the solid and gas hydrate phases; then a medium 2 for water-filled sediment from Gassmann's equation, and finally, they time average media 1 and 2 to obtain the velocity of the partially saturated sediment. Lee et al. (1996) propose that the interval velocity for hydrated deep marine sediment can be estimated from a weighted mean of the three-phase time average equation and the three-phase Wood equation (Wood, 1941). Recently, two mechanical schemes of hydrated deposition in the pore space were proposed (Ecker et al., 1998). In the first scheme, the hydrate may cement grain contacts, which are the weakest structural components of the granular frame. In the second case, the gas hydrate is deposited away from the grain contacts; so, it only weakly affects the stiffness of the granular frame.

In this paper, I use Domenico's approach (Domenico, 1977) to model the acoustic properties of the different layers related to the BSR. The aim is to quantify the concentrations of gas hydrate and free gas in the pore space.

The concentrations can be estimated by fitting theoretical velocity to the experimental velocity, obtained from traveltime inversion or from sonic logs. Positive anomalies indicate the presence of gas hydrate and negative anomalies the presence of free gas. In the following, the method is tested against sonic log and VSP data and indirect estimations of gas hydrate concentration from chloride content in core logs (Paull et al., 1996).

2. The velocity model

The compressional and shear wave velocities can be expressed as

$$V_p = \left\{ \left[\left(\frac{1}{C_m} + \frac{4}{3}\mu \right) + \frac{\frac{\phi_{eff}}{k}\frac{\rho_m}{\rho_f} + \left(1 - \beta - 2\cdot\frac{\phi_{eff}}{k}\right)\cdot(1-\beta)}{(1-\phi_{eff}-\beta)C_b + \phi_{eff}C_f} \right] \cdot \frac{1}{\rho_m\left(1 - \frac{\phi_{eff}}{k}\frac{\rho_f}{\rho_m}\right)} \right\}^{1/2}, \qquad (1)$$

and

$$V_s = \left[\frac{\mu}{\rho_m \left(1 - \frac{\phi_{eff}}{k} \frac{\rho_f}{\rho_m} \right)} \right]^{1/2} \tag{2}$$

respectively (Domenico, 1977). The symbols are explained in Appendix 1.

I apply these equations to three different situations:

1. full water saturation;
2. water and gas hydrates in the pore space;
3. water and gas in the pore space.

I assume that the composite fluid and solid compressibilities lie between the Voigt and Reuss averages (Schön, 1996). They are given by

$$C_f = \frac{1}{2} \cdot \left(s_w \cdot C_w + s_g \cdot C_g \right) + \frac{1}{2} \cdot \left(\frac{s_w}{C_w} + \frac{s_g}{C_g} \right)^{-1}, \tag{3}$$

$$C_b = \frac{1}{2} \cdot \left(s_s \cdot C_s + s_h \cdot C_h \right) + \frac{1}{2} \cdot \left(\frac{s_s}{C_s} + \frac{s_h}{C_h} \right)^{-1}, \tag{4}$$

respectively.

The pore compressibility C_p can be derived from a pore volume empirical function (Domenico, 1977) or, alternatively, from the definition of the compressibility (e.g.,Handbook of Chemistry and Physics, 1992).

To take into account the effects due to the cementation of the grains at high concentrations of gas hydrate, I use a percolation model (Leclaire, 1992). The percolation theory describes the transition of a system from the continuous state (grains completely cemented) to the discontinuous state (uncemented grains). During this process, connections appear or disappear among the elements of the system. The induced modifications of the system configuration are governed by a general power law, in such way that shear modulus of the matrix takes the form

$$\mu_{sm} = \left[\mu_{smKT} - \mu_{sm0} \right] \left[\phi_h / \left(1 - \phi_s \right) \right]^{3.8} + \mu_{sm0} \tag{5}$$

where μ_{smKT} is Kuster and Toksöz's shear modulus (Kuster and Toksöz, 1974) and μ_{sm0} is the shear modulus without cementation (no gas hydrate). This equation models the increasing stiffness of marine sediments with the increasing gas hydrate concentration (Carcione and Tinivella, 1999).

Finally, the coupling factor k describes the degree of coupling between pore fluid and frame. It ranges from one (no coupling) to infinity (perfect coupling) and is related to the frequency of elastic waves. Note that when the coupling factor between the pore fluid and the solid matrix is perfect (zero-frequency case), the velocities are independent of frequency

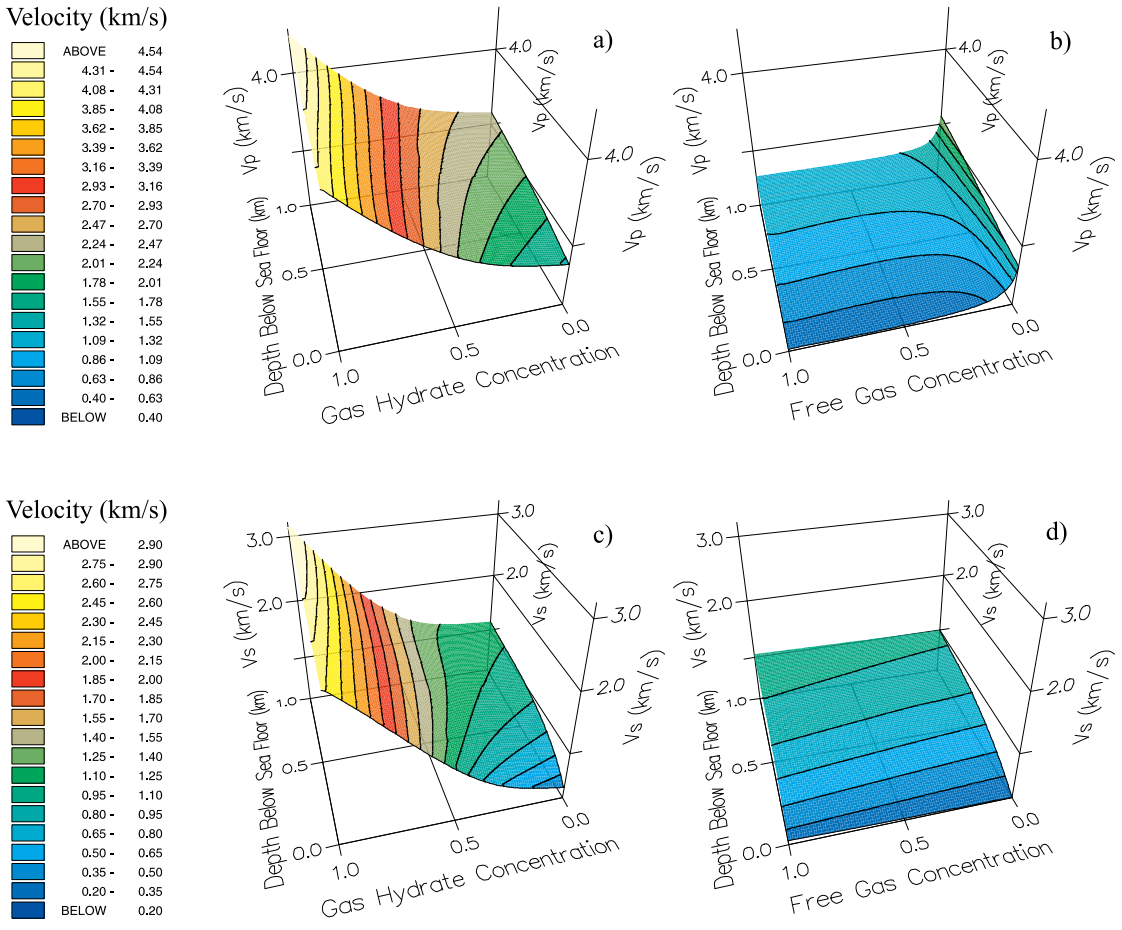

Fig. 1 - Top: Calculated compressional wave velocity for gas hydrate-bearing (a) and free gas-bearing (b) sediments versus depth and clathrate and free gas concentrations. Bottom: Calculated shear wave velocity for gas hydrate-bearing (c) and free gas-bearing (d) sediments versus depth and gas hydrate and free gas concentrations.

(Domenico, 1977).

3. Examples

In order to use equations 1 and 2 for evaluating gas hydrate and free gas concentrations, it is necessary to know the variations of the material properties versus depth. I assume that the compressibilities and densities of the solid components are constant.

Figure 1 shows the calculated compressional and shear velocities for gas-hydrate and free-

gas-bearing sediments versus depth and gas hydrate and free gas concentrations. The values of the parameters for normally compacted terrigenous sediments are given in Appendix B. I assumed that height of the water column is h=2 km and k=∞.

When the hydrate and free gas concentrations are zero, the velocity is that of the water-filled sediment. As expected, both velocities V_p and V_s increase as the gas hydrate concentration increases, particularly for large amounts of gas hydrate. On the other hand, the compressional velocity increases for high free gas concentration, since the density decreases faster than the compressibility.

4. Lee et al.'s model for hydrated sediments

Lee et al. (Lee et al., 1996) proposed that the interval velocity for hydrated deep marine sediment can be estimated from a weighted mean of the Pearson et al. (1983) three-phase time average equation and the three-phase Wood equations (Wood, 1941), following the approach of Nobes et al. (1986). This weighted mean of equations can be written as

$$\frac{1}{V_p} = \frac{W\phi\left(1-c_h\right)^n}{V_{p1}} + \frac{1-W\phi\left(1-c_h\right)^n}{V_{p2}}. \tag{6}$$

V_{p1} is the compressional velocity by the Wood equation given by

$$\frac{1}{\rho_m V_{p1}^2} = \frac{\phi_w}{\rho_w V_w^2} + \frac{\phi_h}{\rho_h V_h^2} + \frac{\phi_s}{\rho_s V_{sm}^2} \tag{7}$$

where V_w is the compressional velocity of water, V_h is the compressional velocity of pure hydrate, and V_{sm} is the compressional velocity of the matrix. V_{p2} is the compressional velocity by the time-average equation

$$\frac{1}{V_{p2}} = \frac{\phi_w}{V_w} + \frac{\phi_h}{V_h} + \frac{\phi_s}{V_{sm}}. \tag{8}$$

W is a weighting factor and n is a constant simulating the rate of lithification with hydrate concentration.

The weight W is only a function of velocity and porosity, but it has an implicit relationship with depth, because the porosities and velocities of sediments depend on depth. For the parameter n, when the hydrates are disseminated throughout the pore space, the lower n such as n=1 may be better suited for the velocity computation. On the other hand, if the hydrates are layered or, selectively cement grains, then a larger n may be applicable.

5. Comparison with experimental data

The methodology is tested by using experimental data obtained during the Leg 164 of the Ocean Drilling Program (ODP) in the Blake Ridge area, offshore South Carolina. Seismic data collected in this area revealed a high amplitude BSR (Paull et al., 1996). Three wells (Sites 994, 995, and 997) penetrated the gas hydrate zone and the free gas zone below the BSR.

The velocity trend derived from in situ measurements (sonic logs) and the VSP profiles can be compared to the theoretical velocity for water-filled sediments. Significant positive deviations between these curves can be related to the presence of clathrates and negative deviations can be associated to free gas-bearing sediments.

For computing the theoretical velocity, I use the porosity and density trends measured in the laboratory at the three sites (Paull et al., 1996), instead of downhole logging measurements. Core-measured densities are generally greater than the downhole logging values at the three Blake Ridge sites (Paull et al., 1996), contrary to typically observed results, which yield lower laboratory values, because the elastic rebounds affecting the sediments specimens after recovery. This discrepancy has been attributed to the degraded borehole conditions at the three sites. I assume that the compressibility of the Blake Ridge sediments (C_s) is equal to $1.34X10^{-11}$ Pa^{-1}, in accordance with the lithologic core characteristics. The rigidity of the sediments, not available from the ODP Leg 164 data set, is extracted from Hamilton's data set (Appendix 2).

A coupling factor equal to three is obtained by fitting the theoretical velocity to the experimental velocity in the zone without gas hydrate and free gas. Figure 2 compares the theoretical velocity (equation 1; solid line) and Lee et al.'s velocity (equation 6; dashed line) to the sonic log velocity (dotted line) and the VSP-derived velocity (dashed-dottedline) versus depth at the three Blake Ridge sites.

The Lee et al.'s velocity is obtained from Eq. (6) assuming n equal to 1 and W=1.5z+0.3 at site 994, W=1.5z+0.35 at site 995, and W=1.5z+0.23 at site 997.

As stated above, the discrepancies between the experimental and theoretical velocities can be translated in terms of concentrations of gas hydrates and free gas. Positive/negative velocity anomalies imply the presence of gas hydrate/free gas with variable concentration in the pore space. In order to as certain the amount of clathrates/free gas in the sediments, I progressively increase the concentrations c_h and s_g, respectively, until they fit the experimental velocity curve.

An indirect measurement of gas hydrate concentration can be obtained from the amount of interstitial-water chloride concentration. During the formation of gas hydrate,water and methane are removed from the pore waters, leaving increasingly saline residuals. Over time, locally elevated chloride concentrations, associated with gas hydrate formation, diffuse. When gas hydrates decompose during drilling and core recovery, they release water and gas back into the pore space, freshening the pore waters. The chloride anomalies are calculated from the differences between the in situ chloride amounts and a fit smooth chloride data c_{fit} (Ussler III and Paull, 1995). The amount of gas hydrate c_h, such as the concentration of dissolved ion Cl^- decrease, can be computed from:

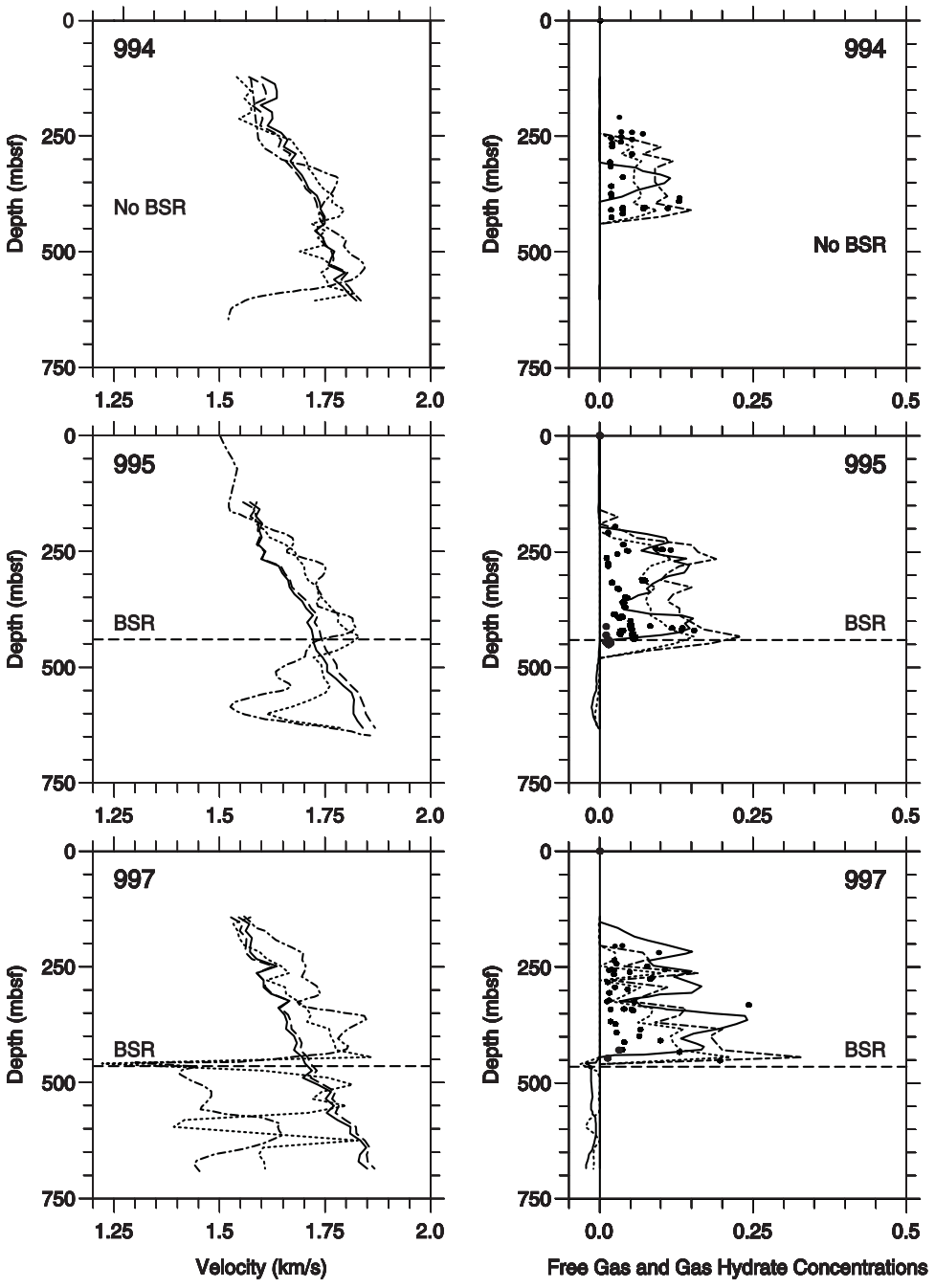

Fig. 2 - Left: Comparison between the theoretical velocity for water-filled sediments (solid line) and Lee et al.'s velocity (dashed line) to the corresponding downhole logging (dotted line) and VSP-derived (dashed-dotted line) velocities,versus depth at the three Blake Ridge sites. Right: Comparison between my predicted concentrations (positive and negative dotted/solid lines correspond to gas hydrate and free gas concentration respectively, considering downhole logging/VSP-derived velocities) and predicted concentrations of gas hydrate (considering downhole logging velocities; dashed line) according to Lee et al. (1996) to the corresponding observed values (dots),versus depth at the three Blake Ridge sites. The observed concentrations are obtained from the amount of interstitial-water chloride concentration (Paull et al., 1996).

$$c_h = \frac{c_{fit} - c_{Cl^-}}{c_{fit}} \tag{9}$$

where c_{fit} is the fitted chloride content, calculated in the absence of clathrates, and c_{Cl^-} is the chloride measurement, assuming that the chloride anomalies are solely due to gas hydrate decomposition during core recovery.

Figure 2 compares my theoretical concentrations (positive dotted line) and Lee et al.'s concentrations (dashed line) of gas hydrate c_h and my theoretical concentrations of free gas s_g (negative dotted line) estimated considering the downhole logging velocities with the corresponding experimental curves (dots) versus depth at the three Blake Ridge sites. The solid lines in Figure 2 indicate the amount of gas hydrate (positive values) and free gas (negative values) estimated considering the discrepancy between the VSP-derived and the theoretical velocities evaluated with equation 1. No experimental profiles are available for free gas concentration. As can be seen, the prediction in my model (dotted and solid lines) is very close to the measured in situ values. The pore-space concentration of gas hydrate estimated from the deviation of the theoretical velocity from the VSP-derived velocity is better at sites 995 and 997, while at site 994 the downhole logging velocity gives the most suitable estimation of gas hydrate quantities.

Quantitative differences between the theoretical and experimental concentration curves for gas hydrate depend mainly on two factors. The first is related to the rigidity and the compressibility in the calculation of the theoretical velocity, which are difficult to measure and which significantly influence the results. The second is related to some experimental errors in the hydrate concentration, in the downhole logging and the VSP-derived velocities, which are fundamental to estimate the concentrations.

Gas volume determinations (deploying Pressure Core Sampler) revealed that the pore space contains more than 12% of gas bubbles in the free gas zone beneath the BSR, assuming gas existing in oversaturated pore water (Dickens et al., 1997). This discrepancy is probably due to a more random gas distribution in the pore space (Domenico, 1977). Moreover, the downhole logging and the VSP-derived velocities are not very accurate in the free gas zone due to poor borehole conditions.

On the other hand, the results indicate that Lee et al.'s model reproduces the correct trend, but overestimates the gas hydrate concentration. So, the accuracy of estimating the hydrate concentration with this model is not good. The author reaches the same conclusion when applying the theory to permafrost (Lee et al., 1996).

6. Conclusions

I developed a simple method to estimate the concentrations of gas hydrate and free gas in marine sediments. The model includes an explicit dependence on differential pressure and depth, and it takes into account the effects of cementation by hydrate on the shear modulus of the sediment matrix. So, it is possible to model the transition between low (no cementation) and high

(cementation) gas hydrate concentration. Moreover, the theory gives both compressional and shear wave velocities, models the existence of two solids (grains and clathrates) and two fluids (water and free gas), and, finally, needs easy to hypothesize parameters.

The technique was successfully tested with a sonic log and core data available at three wells offshore South Carolina. When only seismic data are available, the procedure consists essentially in two steps. In the first step, the acoustic velocity profile is obtained from high resolution seismic analysis (e.g., traveltime tomography). The second step consists in estimating the concentrations by fitting the theoretical velocities to the experimental velocities.

Acknowledgments. I thank José M. Carcione for useful discussions. I am grateful to Angelo Camerlenghi and Emanuele Lodolo for providing the preliminary experimental data. Tim Minshull, Satish C. Singh, and an anonymous reviewer provided valuable advice and thoughtful suggestions. This work was funded by the PNRA (Programma Nazionale di Ricerche in Antartide).

Appendix 1 - List of symbols

ϕ	porosity
ϕ_s	solid proportion
ϕ_h	gas hydrate proportion
ϕ_w	water proportion
ϕ_g	free gas proportion
$\phi_s + \phi_w + \phi_g = 1$	
$\phi_s + \phi_h + \phi_w = 1$	
$c_h = \phi_h / (\phi_h + \phi_w)$	gas hydrate concentration
$s_s = \phi_s / (\phi_{hs} + \phi_h)$	grain saturation
$s_h = \phi_h / (\phi_h + \phi_s)$	gas hydrate saturation
$s_w = \phi_w / (\phi_w + \phi_g)$	water saturation
$s_g = \phi_g / (\phi_w + \phi_g)$	free gas saturation
$\phi_{eff} = (1 - c_h) \cdot \phi$	effective porosity
C_s	grain compressibility
C_h	gas hydrate compressibility
C_w	water compressibility
C_g	free gas compressibility
C_b	average compressibility of the solid phase
C_f	average compressibility of the fluid phase
C_p	pore compressibility

$C_m = \left(1-\phi_{eff}\right)\cdot C_b + \phi_{eff}\cdot C_p$	compressibility of the matrix
$\beta = C_b / C_m$	
μ_s	grain rigidity
μ_{sm}	solid matrix shear modulus
μ_h	gas hydrate rigidity
$\mu = \left(\phi_s + \phi_h\right)\cdot\left(\phi_s s_s / \mu_{sm} + s_h / \mu_h\right)^{-1}$	average rigidity of the skeleton
ρ_s	grain density
ρ_h	gas hydrate density
ρ_w	water density
ρ_g	free gas density
$\rho_b = s_s\cdot\rho_s + s_h\cdot\rho_h$	density of the solid phase
$\rho_f = s_w\cdot\rho_w + s_g\cdot\rho_g$	density of the fluid phase
$\rho_b = \left(1-\phi_{eff}\right)\cdot\rho_b + \phi_{eff}\cdot\rho_f$	average density
k	coupling factor

Appendix 2 - Variations of the material properties versus depth

$[z] = \mathrm{m}$	
$\phi = 0.72 - 816.5z + 361z^2$	terrigenous sediments (Hamilton, 1976a)
$C_s = 2.7\times10^{-11}\,\mathrm{Pa}^{-1}$	quartz (Zimmerman and King, 1986)
$C_h = 1.79\times10^{-10}\,\mathrm{Pa}^{-1}$	pure hydrate (Sloan, 1990)
$C_w = -9.5\times10^{-15}\,\mathrm{Pa}^{-2}\,p(z) + 4.63\times10^{-10}\,\mathrm{Pa}^{-1}$	Riley and Chester (1987)
$p(z) = p_{atm} + \left[\int_0^h \rho_w(z')dz'\right]g + \left[\int_0^z \rho_w(z')dz'\right]g$	pressure
p_{atm}	pressure of the atmosphere
h	height of the water column
$C_g = 4.24\times10^{-8}\,\mathrm{Pa}^{-1}$	methane (Handbook of Chemistry and & Physics, 1992)
$\rho_m = 1530 + 1395z - 617z^2\ \mathrm{kg/m^3}$	terrigenous sediments (Hamilton, 1976a)
$V_s = 116 + 4.65z\ \mathrm{m/s},\ z < 36\mathrm{m}$	
$V_s = 237 + 1.28z\ \mathrm{m/s},\ 36\mathrm{m} < z < 120\mathrm{m}$	terrigenous sediments (Hamilton, 1976b)
$V_s = 322 + 0.58z\ \mathrm{m/s},\ z > 120\mathrm{m}$	

$\mu_{sm0} = \rho_m (V_s)^2 [\text{Pa}]$	shear modulus without cementation
$\mu_h = 2.4 \times 10^9 \text{ Pa}$	pure hydrate (Sloan, 1990)
$\rho_s = 2650 \text{ kg/m}^3$	quartz (Zimmerman and King, 1986)
$\rho_h = 767 \text{ kg/m}^3$	pure hydrate (Sloan, 1990)
$\rho_g = 88.48 \text{ kg/m}^3$	methane (Handbook of Chemistry and Physics, 1992)
ρ_w	empirical formula (Fofonoff and Millard, 1983)
density of sea water 1040 kg/m^3	(Fofonoff and Millard, 1983)
temperatue of sea water 0.1 °C	(Fofonoff and Millard, 1983)
salinity of sea water 35	(Fofonoff and Millard, 1983)
geothermical gradient 0.03 °C/m	(Fofonoff and Millard, 1983)

References

Carcione J. M. and Tinivella U.; 1999: *Bottom simulating reflectors: seismic velocities and AVO effects.* Geophysics, in press.

Claypool G. E. and Kaplan I. R.; 1974: *Methane in marine sediments.* In: Kaplan, I. R. (ed), Natural Gases in marine sediments, pp. 99-139.

Dickens G. R., Paull C. K., Wallace P. and the ODP Leg 164 Scientific Party; 1997: *Direct measurements of in situ methane quantities in a large gas-hydrate reservoir.* Nature, **385,** 426-428.

Domenico S. N.; 1977: *Elastic properties of unconsolidated porous sand reservoirs*. Geophysics, **42,** 1339-1368.

Ecker C., Dvorkin J. and Nur A.; 1998: *Structure of hydrated sediments from seismic and rock physics.* Geophysics, **63,** 1659-1669.

Fofonoff N. P. and Millard R. C. Jr.; 1983: *UNESCO Technical Papers in Marine science.* **44,** 1983.

Hamilton E. L.; 1976a: *Variations of density and porosity with depth in deep-sea sediments.* Journal of Sedimentary Petrology, **46,** 280-300.

Hamilton E. L.; 1976b: *Shear-wave velocity versus depth in marine sediments: a review*. Geophysics, **41,** 985-996.

Handbook of Chemistry and Physics; 1992. Chemical Rubber Co. Press, Cleveland.

Kuster G. T. and Toksöz M. N.; 1974: *Velocity and attenuation of seismic waves in two-phase media: Part I. Theoretical formulations*. Geophysiscs, **39,** 587-606.

Leclaire P.; 1992: *Propagation acoustique dans les milieux poreux soumis au gel-Modélisation et expérience*. Thèse de Doctorat en Physique, Université Paris 7, Paris.

Lee M. W., Hutchinson D. R., Collet T. S. and Dillon W. P.; 1996: *Seismic velocities for hydrate-bearing sediments using weighted equation.* Journal of Geophysical Research, **101,** 20347-20358.

Minshull T. A., Singh S. C. and Westbrook G. K.; 1994: *Seismic velocity structure at the gas hydrate reflector, offshore western Colombia, from full waveform inversion.* Journal of Geophysical research, **99,** 4715-4734.

Nobes D. C., Villenger H., Davis F. F. and Law L. K.; 1986: *Estimation of marine sediment bulk physical properties at*

depth from seafloor geophysical measurements. J. Geophys. Res., **91,** 14033-14043.

Paull C. K., Matsumoto R., Wallace P. J. et al.; 1996: *Proceedings of the Ocean Drilling Program*. Initial Reports. Texas A&M Univ., College Station, TX, 164.

Pearson C. F., Halleck P. M., McGulre P. L., Hermes R. and Mathews M.; 1983: *Natural gas hydrate; A review of in situ properties.* J. Phys. Chem., **87,** 4180-4185.

Reuss A.; 1929: *Berechnung der Fleissgrenze von Mischkristalen auf Grund der Plastizitäts belingung für ein Kristalle, Z. Angew.* Math. Mech., **9,** 49-58.

Riley J. P. and Chester R.; 1987: *Introduction to Marine Chemistry.* Accademic Press, London, pp. 465.

Schön J. H.; 1996: *Physical properties of rocks. Fundamentals and principles of petrophysics*. Pergamon Press, Oxford, pp. 583.

Shypley T. H., Houston M. H., Buffler R. T. et al.; 1979: *Seismic reflection evidence for widespread occurrence of possible gas-hydrate horizons on continental slopes and rises.* AAPG Bulletin, **63,** 2204-2213.

Sloan E. D.; 1990: *Clathrate hydrates of natural gas.* Marcel Dekker, New York, pp.641.

Timur A.; 1968: *Velocity of compressional waves in porous media at permafrost temperatures.* Geophysics, **33,** 584-595.

Ussler III W. and Paull C. K.; 1995: *Effects of ion axclusion and isotopic fractionation on pore water geochemistry during gas hydrate formation and decomposition.* Geo-marine Letters, **15,** 37-44.

Voigt W.; 1928: *Lehrbuch der Kristallphysik*. B. G. Terbner, Leipzig.

Wood A. B.; 1941: *A text book of sound.* Macmillan, New York.

Zimmerman R. W. and King M. S.; 1986: *The effect of the extent of freezing on seismic velocities in unconsolidated permafrost.* Geophysics, **51,** 1285-1290.